Biochimica et Biophysica Acta, 548 (1979) 139—146

BBA 47737

EXCHANGE INTEGRAL FOR A VARIETY OF TETRANUCLEAR FERREDOXINS

HAYWOOD BLUM, J.C. SALERNO *, PETER R. RICH ** and TOMOKO OHNISHI

Johnson Research Foundation, Department of Biochemistry and Biophysics, School of Medicine, University of Pennsylvania, Philadelphia, PA 19104 (U.S.A.)

(Received February 2nd, 1979)

Key words: Iron-sulfur protein; Ferredoxin; Antiferromagnetic exchange; Tetranuclear ferredoxins; (ESR)

Summary

The temperature dependence of EPR spectra of oxidized $[4Fe\text{-}4S^*]^{(-1,-2)}$ ferredoxins (previously designated HiPIP) and a reduced $[4Fe\text{-}4S^*]^{(-2,-3)}$ ferredoxin have been analyzed so as to determine the energy of a low-lying excited electronic state. The values obtained were: Center S-3 from beef heart, 44 cm^{-1}; Center S-3 from mung bean, 53 cm^{-1}; the $[4Fe\text{-}4S^*]^{(-1,-2)}$ ferredoxin from *Thermus thermophilus*, 78 cm^{-1}; Center N-2 of NADH ubiquinone reductase, 83 cm^{-1}. Increasing axial distortion in the EPR spectra of the $[4Fe\text{-}4S^*]^{(-1,-2)}$ ferredoxins was associated with higher energy differences. Center N-2, a $[4Fe\text{-}4S^*]^{(-2,-3)}$ iron-sulfur cluster does not fit this relationship.

Introduction

Recently, we reported [1] a study of the temperature dependence of the electron paramagnetic resonance (EPR) spectra of a number of reduced binuclear ferredoxins $[2Fe\text{-}2S^*]^{(-2,-3)}$. We were able to relate the increase in EPR linewidth and the fall-off of the EPR integrated intensity to a low-lying excited state which could be interpreted in terms of antiferromagnetic exchange coupling between the two iron ions.

* Present address: Department of Biochemistry, Duke University School of Medicine, Durham, NC 27710, U.S.A.

** Present address: Department of Biochemistry, University of Cambridge, Tennis Court Road, Cambridge CB2 1QW, U.K.

Abbreviation: HiPIP, high potential iron-sulfur protein, is an abbreviation for a class of iron sulfur-proteins which are paramagnetic in their oxidized form.

In this paper we report similar measurements on tetranuclear iron-sulfur proteins which are either paramagnetic in the oxidized form $[4Fe\text{-}4S^*]^{(-1)}$ (formerly known as *Chromatium* HiPIP types) or in the reduced form $[4Fe\text{-}4S^*]^{(-3)}$ (previously called clostridial ferredoxin types) [2]. We find that the EPR spectral parameters can be related to the electronic structure of the ferredoxin in a regular way.

The integrated intensity of the EPR spectrum can be used to locate nearby excited states. As the EPR visible state becomes thermally depopulated its total magnetism falls off faster than predicted from the simple Curie law temperature dependence. Thus [1,3],

$$(I \cdot T) = (I \cdot T)_{LT} \cdot (1 + me^{-\Delta/kT})^{-1}$$

where Δ is the position of the excited state, m is its multiplicity relative to the ground state, I is the integrated intensity of the EPR spectrum, and the subscript LT means low temperature, that is, a temperature at which the product $I \cdot T$ has become constant.

The analysis of the EPR line width so as to elicit the Lorentzian spin packet spin-lattice relaxation time, T_1, is described in the Results. The dependence of T_1 on temperature follows an Orbach process [3–5]:

$$T_1^{-1} = A(e^{\Delta/kT} - 1)^{-1}$$

and for $\Delta/kT >> 1$

$$T_1^{-1} = Ae^{-\Delta/kT}$$

Materials and Methods

EPR techniques and equipment have been described previously [1,3]. Reconstitutively active soluble succinate dehydrogenase was prepared as described in Ref. 6. Membrane-bound succinate dehydrogenase from mung bean hypocotyls (*Phaseolus aureus*) was prepared by the method of Rich and Bonner [7]. NADH ubiquinone reductase was prepared by the method of Hatefi et al. [8].

The [4Fe-4S*] center from *Thermus thermophilus* HB8 was a gift from Dr. T. Oshima. Its purification will be described elsewhere (Sato, S. et al., unpublished).

Results

Center S-3

Fig. 1 shows the EPR derivative spectra of Beef heart S-3 at various temperatures. The low temperature spectrum was computer simulated and fit with the parameters given in the legend of Fig. 1, equal to those of Ruzicka et al. [9], except that the line widths were slightly larger. In this preparation a $g = 2$ signal becomes a large factor as the temperature is raised. In fact, at 32 K (Fig. 1C) the S-3 signal has become so broad as to be almost invisible at the sensitivity necessary to keep the recorder tracing on scale. This free radical type signal has a peak-to-peak line width of 1.6 mT (16 gauss), too wide to be a quinone

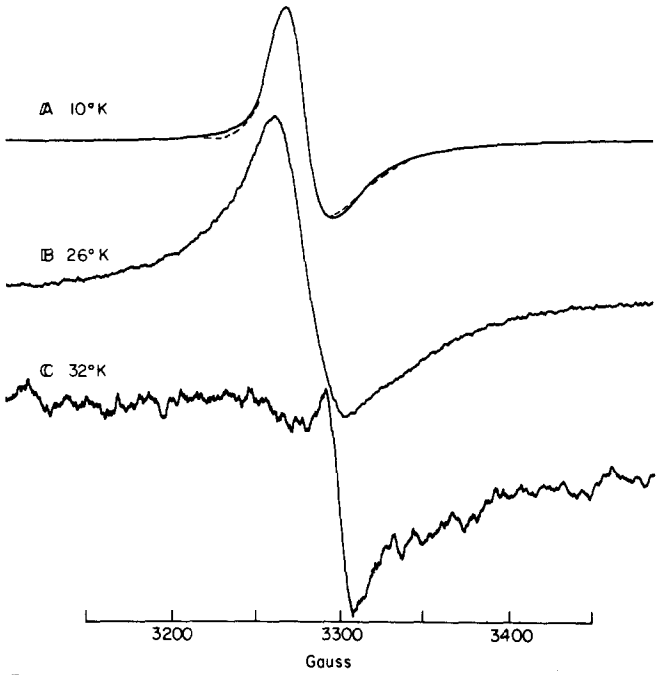

Fig. 1. EPR spectra of center S-3 of succinate-cytochrome *c* reductase from beef heart taken at 20 mW of incident power (solid curves). Computer simulation, dashed curve. EPR parameters assumed for simulation: $g_x = 1.990$, $g_y = 2.0108$, $g_z = 2.0190$; $\Delta H_x = 2.6$ mT (26 gauss), $\Delta H_y = 1.5$ mT (15 gauss), $\Delta H_z = 1.0$ mT (10 gauss), where the Gaussian line width ΔH varies with g value according to the expression $\Delta H = (\Delta H_x^2 1_x^2 + \Delta H_y^2 1_y^2 + \Delta H_z^2 1_z^2)^{1/2}$ and 1_x, 1_y, 1_z are the direction cosines between the external magnetic field and the principal g-axes.

radical alone. It may arise from a flavin; however, the flavin of SDH is not paramagnetic in the fully oxidized form.

This difficulty at higher temperature is obviated by using integrals of these spectra, as shown in Fig. 2. The area under the narrow $g = 2$ signal is actually small compared to that under the S-3 signal and makes a slight overall contribution.

Line widths could be taken from the asymmetric integrals as shown in Fig. 2C. ΔH is the distance from the line center to the half height on the low field side. This is a somewhat arbitrary but nonetheless useful way of deriving a line width. This parameter is plotted in Fig. 3 (closed circles) as a function of inverse temperature.

To extract the line width of individual spin packets from information about the overall line width the approximate expression, $\Delta H^2 = \Delta H_L^2 + \Delta H_G^2$, was used, where ΔH_G is the low temperature inhomogeneous (Gaussian) line width, and ΔH_L is the (Lorentzian) line width due to the lifetime of the individual spin packets. This expression is strictly correct only for a convolution of Gaussian distributions [10]. The Lorentzian line width so derived is plotted in Fig. 3 (open circles) and one sees that the line width and therefore the inverse spin-lattice lifetime, T_1^{-1}, can be expressed as $T_1^{-1} \propto \Delta H_L \propto \exp(-\Delta/kT)$ with $\Delta = 44.7\ cm^{-1}$.

A more exact determination of the spin packet line widths was made using

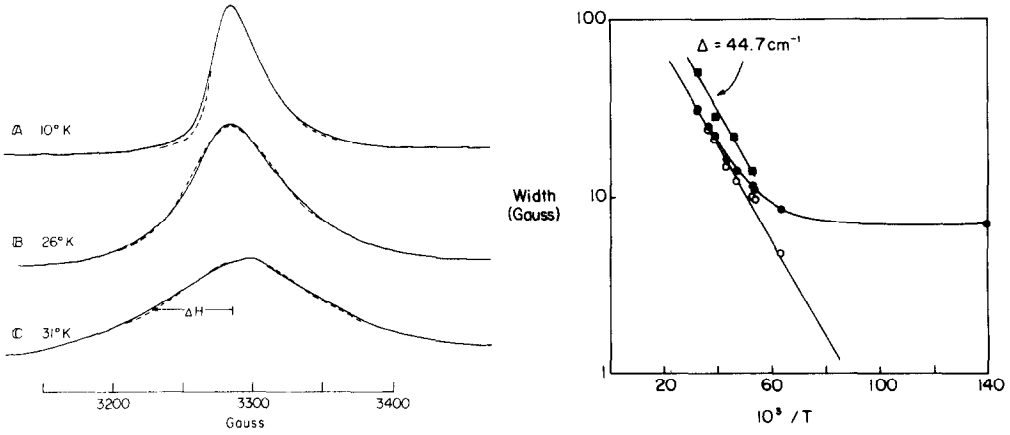

Fig. 2. Integrals of EPR spectra of center S-3 similar to those shown in Fig. 1 (solid curves). Simulations (dashed curves) were made as described in the legend of Fig. 1. The spectra were then braodened by convolution with a Lorentzian line shape whose half-width is: (A) 10 K, 0; (B) 26 K, 2.8 mT (28 gauss); (C) 31 K, 5.0 mT (50 gauss).

Fig. 3. Line width of the EPR absorption spectrum of center S-3 (distance in gauss from the peak position to the half maximum field on the low field side) versus inverse temperature (•). Fit to these data assuming that the spin packet line width ΔH_L can be extracted by $\Delta H_L = (\Delta H^2 - \Delta H_G^2)^{1/2}$ where ΔH_G is the low temperature value of ΔH (○). Line has a slope $\Delta = 44.7$ cm^{-1}. Widths of Lorentzian spin packets needed to fit spectra in Fig. 2 with computer simulations (■).

computer simulations of the EPR absorption spectra. The basic low temperature EPR parameters, given in Fig. 1, were held fixed and were convoluted with Lorentzian spin packets whose width was varied to fit the spectra of Fig. 2 (dashed curves). These line widths are plotted in Fig. 3. The value found for Δ is unchanged.

Integrals of the EPR absorption spectra, I, were digitally obtained. $I \cdot T$, where T is the absolute temperature, are plotted in Fig. 4 versus inverse temperature. The fall-off in intensity with increasing temperature can be fit by assuming an exited state at 43.2 ± 4 cm^{-1} above the EPR visible ground state

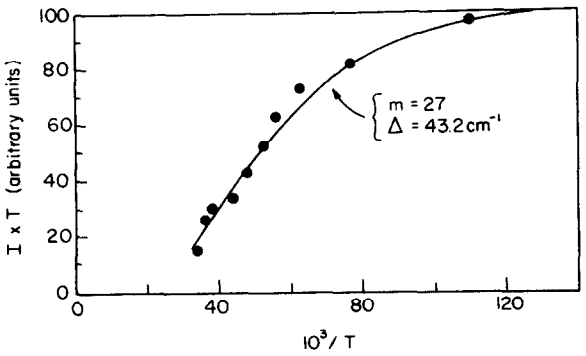

Fig. 4. Integrated absorption of center S-3 times absolute temperature, $I \cdot T$, versus inverse temperature (•). Vertical scale is normalized to $I \cdot T = 100$ at low temperatures. Curve assumes an excited state at $\Delta = 43.2$ cm^{-1} above ground state with relative multiplicity of $m = 27$.

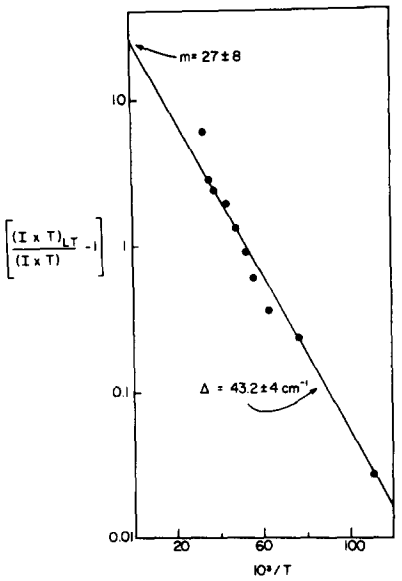

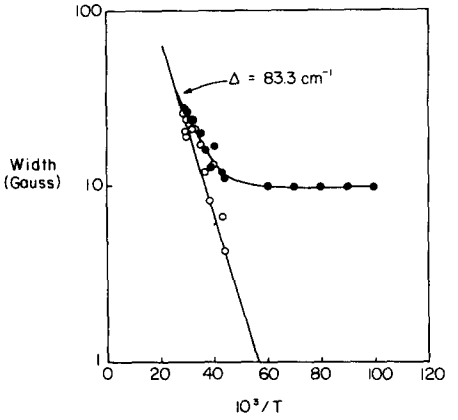

Fig. 5. Data of Fig. 4 for center S-3 replotted (•). Straight line is least-squares fit to data. Slope gives $\Delta = 43.2 \pm 4$ cm^{-1} and y-intercept gives $m = 27 \pm 8$.

Fig. 6. Linewidth of the EPR derivative spectra of center N-2 of NADH ubiquinone reductase from beef heart (distance in G from peak-to-peak of the $g_\perp$ signal) versus inverse temperature (•). Fit of Lorentzian spin packet line width as in Fig. 3 (○). Line has slope $\Delta = 83.3$ cm^{-1}.

with a relative multiplicity of 27 ± 8. In Fig. 5, the data are replotted to show this fit.

The EPR signal from mung bean S-3 [7] was followed to 24 K (data not shown). From analysis of linewidth and intensity data we find $\Delta = 53 \pm 10$ cm^{-1} and $m = 25 \pm 10$.

T. thermophilus

EPR studies of *T. thermophilus* HB8 [4Fe-4S*]$^{(-1,-2)}$ ferredoxin have been reported previously [11]. The center has principal g values in the oxidized state of $g_x = 1.93$, $g_y = 1.98$, $g_z = 2.014$. We find from integrated intensity measurements (data not shown), $\Delta = 78.6 \pm 3$ and $m = 1400 \pm 400$. Other results will be forthcoming (Ohnishi, T. et al., unpublished).

Center N-2

The EPR spectrum of reduced center N-2 is well-known [12,13]. In Fig. 6 we plot the line width of the $g_\perp$ peak versus inverse temperature. In this case the parameter measured was the distance in gauss between the peaks. The data were analyzed in the same way as the S-3 linewidth data. We find $\Delta = 83.3$ cm^{-1}. Signals from other iron-sulfur centers in this preparation made the measurement of the integrated intensity unfeasible.

Discussion

Many of the magnetic and electronic properties of the [2Fe-2S*] ferredoxins can be understood on the basis of a model of antiferromagnetic exchange

coupling between the iron ions [14,15]. This model predicts a ladder of excited states whose spacing depends on the magnitude of the exchange coupling constant J ($J < 0$). The first excited state in the reduced ferredoxin is $-3J$ above the ground state. Except for one example [16] only the first excited state in the ladder has been detected.

In Fig. 7 we show the interrelationship of J for binuclear ferredoxins and the rhombicity of the EPR spectrum. These data have been reported previously [1] except for spinach ferredoxin [9] and are included here for comparison with the tetranuclear case.

The antiferromagnetic model may also be applied to tetranuclear ferredoxins [3]. If the coupling among the iron ions is the same, the ladder of excited states will be the same as in the binuclear case with the first excited state at $\Delta = -3J$ above the EPR visible ground Kramers doublet. Again there is only one measurement at this time [17] in which more than the first excited state has been detected.

Fig. 8 shows the relationship of Δ to the EPR parameter $g_z - g_y$. At first observation the tetranuclear ferredoxins studied appear to have only axial distortion with $g_x = g_y$. This is not actually the case with Center S-3 and the ferredoxin from *T. thermophilus*. The apparent axiality is due mainly to the large line width of the EPR spectra near g_x. Nevertheless, $g_z - g_y$ can be taken as a measure of the axial distortion of the system from tetrahedral symmetry. Fig. 8 shows that this is associated with increasing Δ for the HiPIP types. Center N-2 which is EPR visible when reduced to the $[4Fe\text{-}4S^*]^{(-3)}$ state does not fall on this curve. Thus the HiPIP types of ferredoxin can be distinguished from the clostridial types, such as center N-2 of NADH dehydrogenase [19] on the basis of the EPR parameters and the value of the exchange integral. The relationships summarized in Figs. 7 and 8 are thus useful for sorting out the ferredoxins.

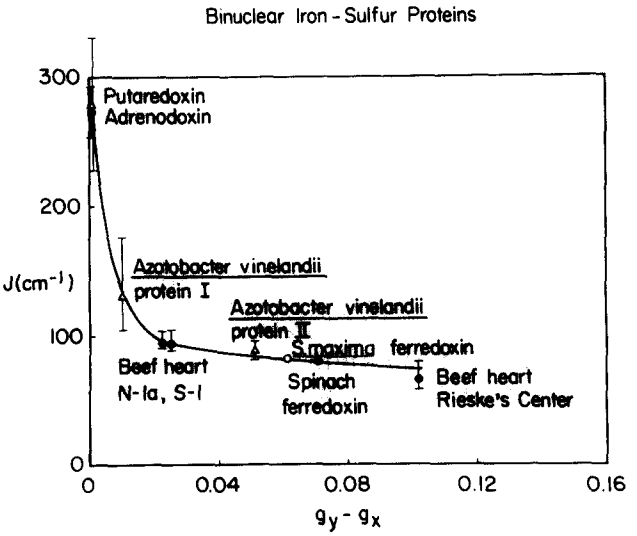

Fig. 7. Relationship between the antiferromagnetic constant J for binuclear ferredoxins and rhombic distortion of the EPR spectrum as measured by $g_y - g_x$. See Refs. 1 and 9.

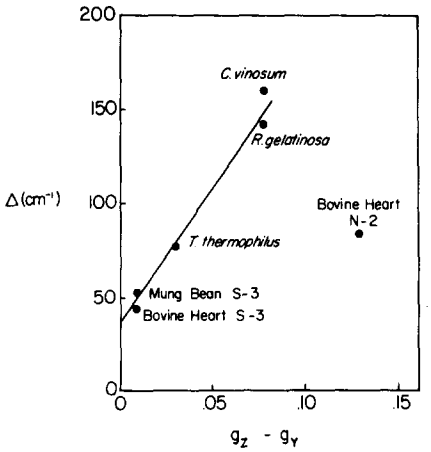

Fig. 8. Relationship between the position of the first excited state of tetranuclear iron-sulfur proteins and the axial distortion of the EPR spectrum as measured by $g_Z - g_Y$. Values for *Chromatium vinosum* and *Rhodopseudomonas gelatinosa* are from Refs. 3 and 17, respectively. g values for *C. vinosum* from Ref. 18.

We note that in similar systems [20] the exchange integrals are extremely sensitive to the distance between the iron ions so that it is at least consistent that increased axiality (especially if it implies a decrease of Fe-Fe distance) correlates with increased Δ.

At this time we are unable to find a connection between the electronic structure as revealed through EPR parameters and physiological information such as the midpoint potentials of these proteins.

Acknowledgments

We would like to thank Dr. T. Oshima for his generous gift of the *T. thermophilus* iron-sulfur protein. We also thank Dr. T.E. King for the Complex I preparation and Dr. B.L. Trumpower for the succinate-cytochrome *c* reductase preparation. This work was supported by N.I.H. grants GM-25052 and GM-12202 and by National Science Foundation grant PCM 75-13459.

References

1 Salerno, J.C., Ohnishi, T., Blum, H. and Leigh, J.S. (1977) Biochim. Biophys. Acta 494, 191—197
2 Cammack, R., Dickson, P.E. and Johnson, C.E. (1977) In Iron-Sulfur Proteins, (Lovenberg, W., ed.), Vol. III, pp. 283—330, Academic Press, New York
3 Blum, H., Salerno, J.C., Prince, R.C., Leigh, J.S. and Ohnishi, T. (1977) Biophys. J. 20, 23—31
4 Orbach, R. (1961) Proc. R. Soc. Lond. A 264, 458—484
5 Gayda, J.P., Gibson, J.F., Cammack, R., Hall, D.P. and Mullinger, R. (1976) Biochim. Biophys. Acta 434, 154—163
6 Ohnishi, T., Salerno, J.C., Winter, D.B., Lim, J., Yu, C.A., Yu, L. and King, T.E. (1976) J. Biol. Chem. 251, 2094—2104
7 Rich, P.R. and Bonner, W.D., Jr. (1978) Biochim. Biophys. Acta 501, 381—395
8 Hatefi, Y., Haavik, A.G. and Griffiths, D.E. (1962) J. Biol. Chem. 237, 1676—1680
9 Ruzicka, F.J., Beinert, H., Schepler, K.L., Dunham, W.R. and Sands, R.H. (1975) Proc. Natl. Acad. Sci. U.S. 72, 2886—2890
10 Coffman, R.E. (1975) J. Phys. Chem. 79, 1129—1136
11 Ohnishi, T., Blum, H., Sato, S., Honnami, K. and Ohshima, T. (1979) Abst. XIth Int. Congr. Biochem.

12 Ohnishi, T. (1975) Biochim. Biophys. Acta 387, 475—490
13 Orme-Johnson, W.H. and Beinert, H. (1969) J. Biol. Chem. 244, 6143—6148
14 Gibson, J.F., Hall, D.O., Thornley, J.F. and Whatley, F. (1966) Proc. Natl. Acad. Sci. U.S. 56, 987–990
15 Blum, H., Leigh, J.S., Ohnishi, T. and Salerno, J.C. (1978) In Frontiers of Biological Energetics (Dutton, P.L., Leigh, J.S. and Scarpa, A., eds.), Vol. I, pp. 625—633, Academic Press, New York
16 Blum, H., Adar, F., Salerno, J.C. and Leigh, J.S. (1977) Biochem. Biophys. Res. Commun. 77, 650–657
17 Blum, H., Salerno, J.C. and Cusanovich, M.A. (1978) Biochem. Biophys. Res. Commun. 84, 1125–1128
18 Antanaitis, B.C. and Moss, T.H. (1975) Biochim. Biophys. Acta 405, 262—279
19 Albracht, S.P.J. and Subramanian, J. (1977) Biochim. Biophys. Acta 462, 36—48
20 Ginsberg, A.P., Lines, M.E., Karlin, K.D., Lippard, S.J. and DiSalvo, F.J. (1976) J. Am. Chem. Soc 98, 6958—6966